

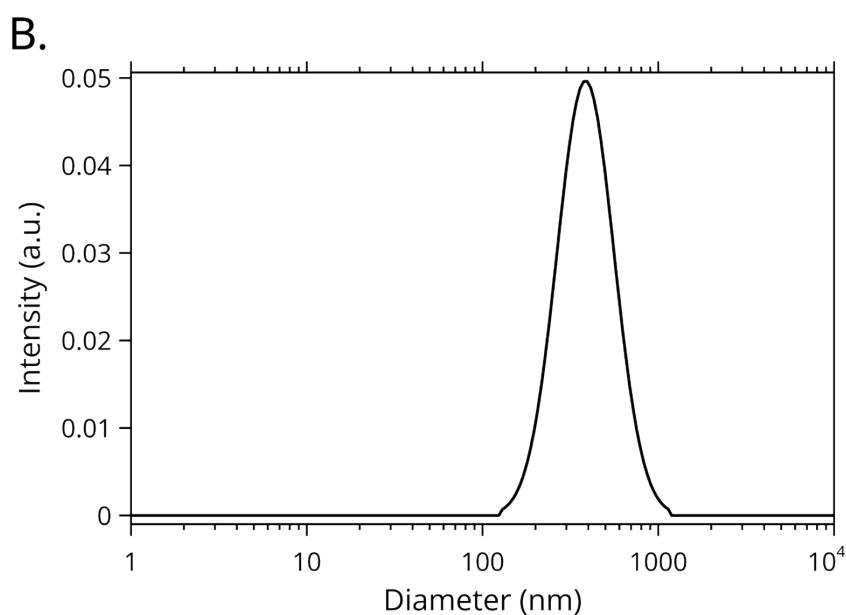
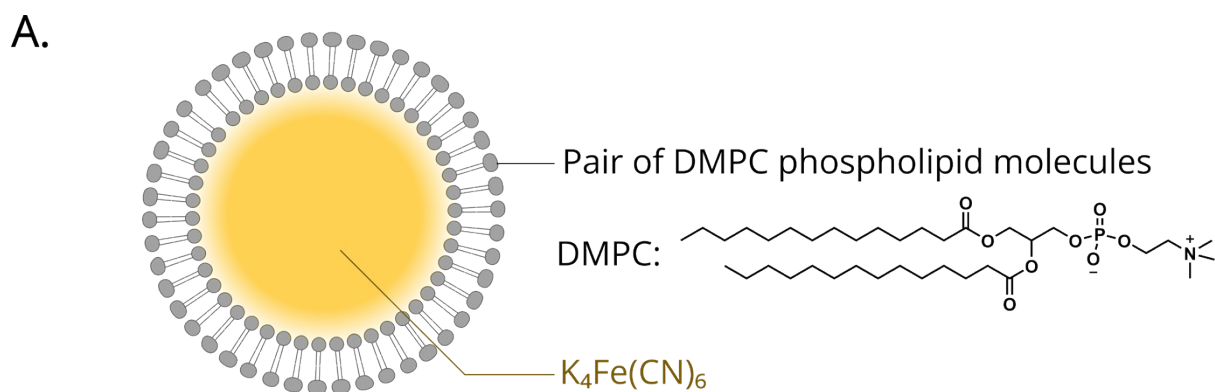
Supporting Information

Microscope observation of united liposome trajectories near a polarized ultramicroelectrode surface

Arthur Langlard,^{*a} Christine Thobie-Gautier,^a Mohammed Boujtita^a and Estelle Lebègue^{*a}

^aNantes Université, CNRS, CEISAM, UMR 6230, F-44000 Nantes, France

*Corresponding authors: Arthur Langlard; <https://orcid.org/0009-0005-6968-0766>; arthur.langlard@univ-nantes.fr and Estelle Lebègue; <https://orcid.org/0000-0002-8610-0891>; estelle.lebegue@univ-nantes.fr



C.

ζ -potential (mV)
3.58
4.62
3.71
4.35
4.87

Fig. S1 A. Composition of the DMPC liposomes used in this study. B. Size distribution of a suspension of redox DMPC liposomes from a dynamic light scattering measurement (a.u.: arbitrary units provided by the instrument). C. ζ -potential values of the synthesized redox DMPC liposomes.

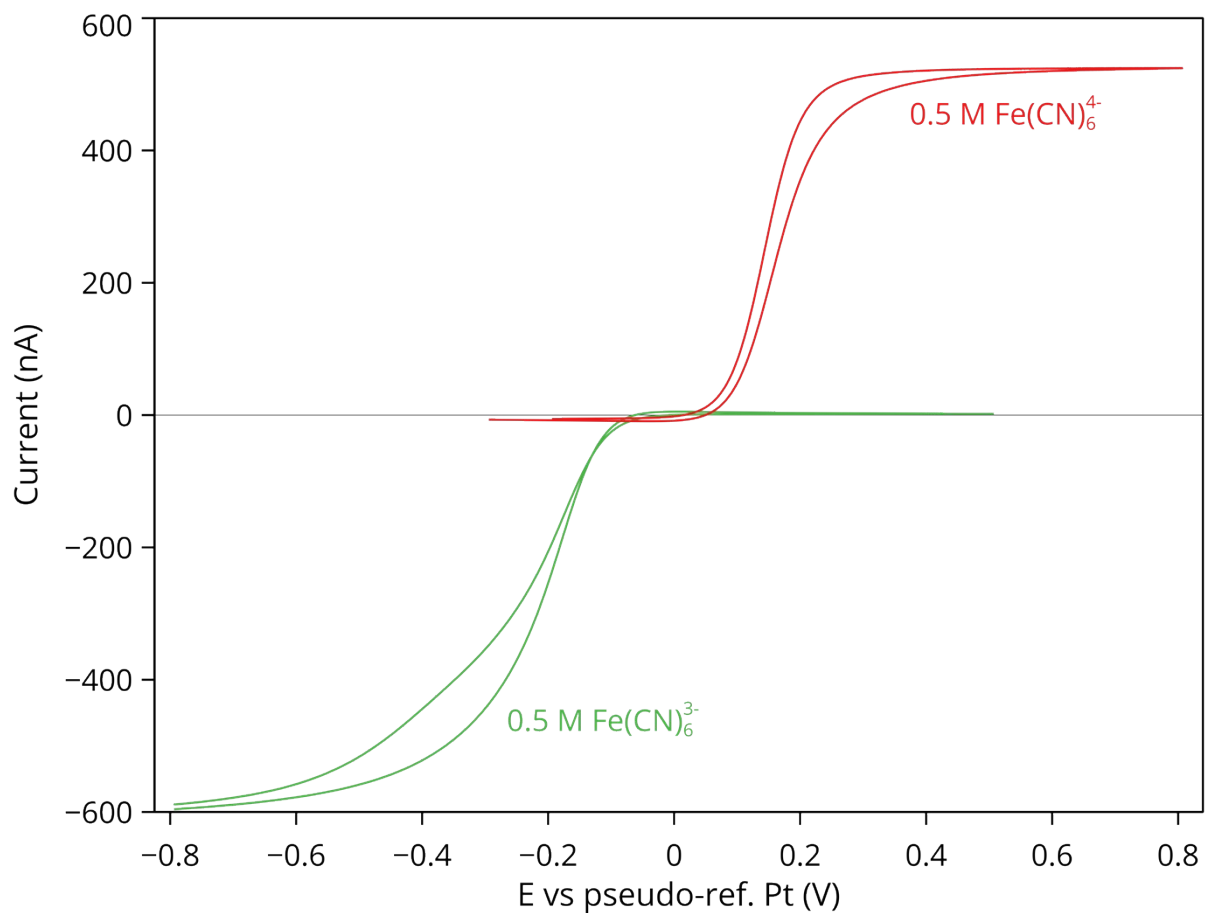


Fig. S2 Cyclic voltammetry of a 0.5 M ferrocyanide solution in 0.1 M PBS recorded at 20 mV s⁻¹ at a 10 μm diameter disk Pt UME (red curve) and cyclic voltammetry of a 0.5 M ferricyanide solution in 0.1 M PBS recorded at 20 mV s⁻¹ at a 10 μm diameter disk Pt UME (green curve). Second cycle is shown.

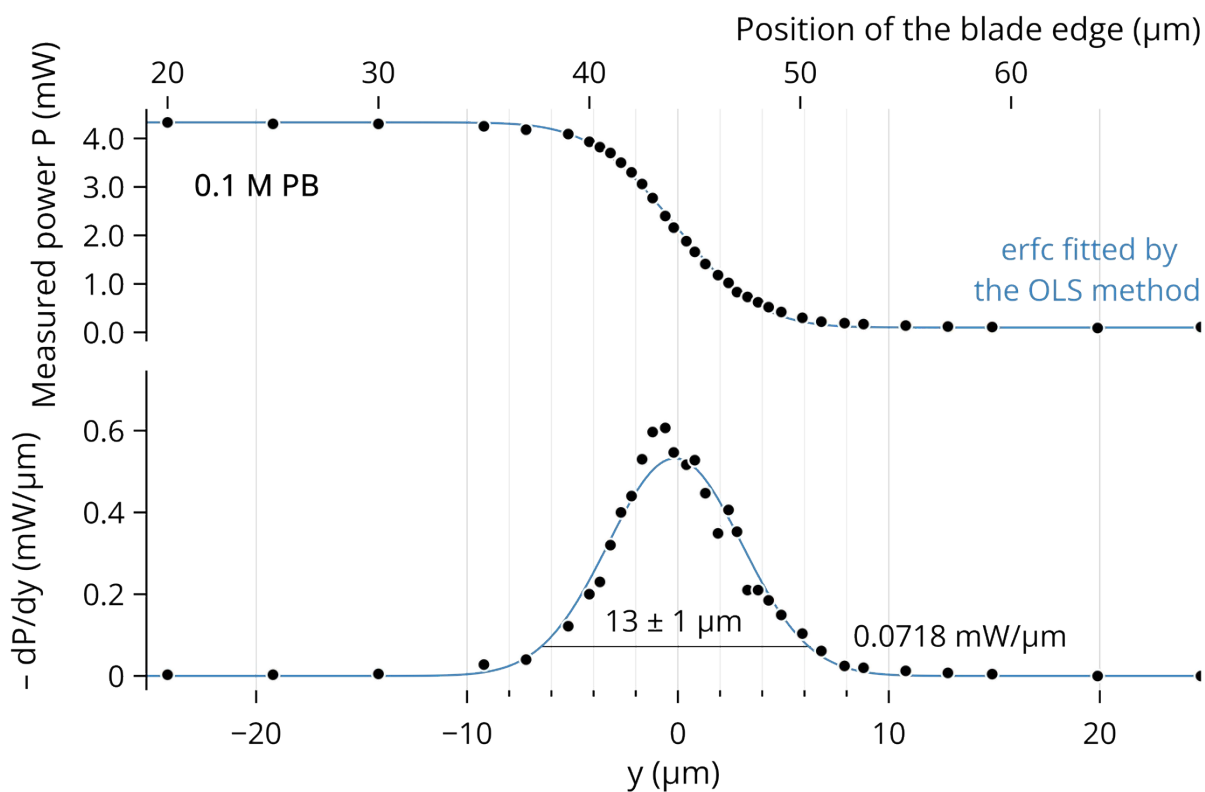


Fig. S3 Profile of the laser beam along its short axis in an aqueous solution of 0.1 M PB. The top horizontal axis relates to the raw measurement of the blade position as read on the micrometer scale, and the bottom horizontal axis is the same measurement shifted to be centered on the Gaussian curve. The measurement uncertainties (not visible) are $\pm 0.2 \mu\text{m}$ for the blade position and $\pm 0.01 \text{ mW}$ for the measured power. The uncertainty in the beam width is estimated at $\pm 1 \mu\text{m}$. OLS: ordinary least squares.

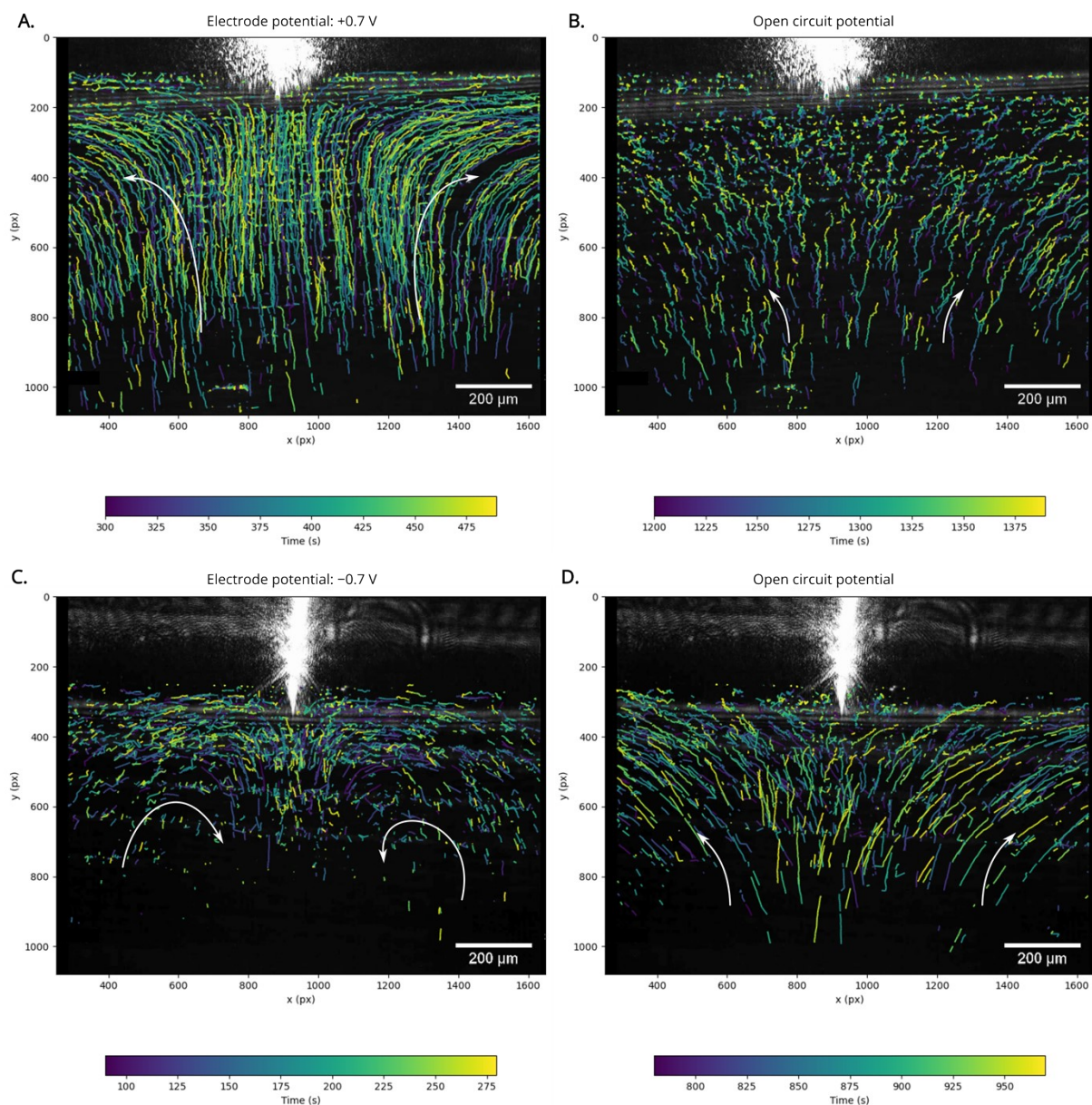


Fig. S4 Trajectories of liposomes in solution under the effect of electrode polarization. The overexposed area at the top of the image is the metal wire of the Pt UME reflecting the laser beam. A. Pt UME polarized at +0.7 V vs. Pt pseudo-ref. in 0.5 M $\text{K}_4\text{Fe}(\text{CN})_6$ dissolved in 0.1 M PB. B. No potential applied (OCP) in 0.5 M $\text{K}_4\text{Fe}(\text{CN})_6$ dissolved in 0.1 M PB. C. Electrode polarized at -0.7 V vs. Pt pseudo-ref. in 0.5 M $\text{K}_3\text{Fe}(\text{CN})_6$ dissolved in 0.1 M PB. D. No potential applied (OCP) in 0.5 M $\text{K}_3\text{Fe}(\text{CN})_6$ dissolved in 0.1 M PB. When no potential is applied to the electrode, the liposomes are transported by an unwanted global convection movement, which is difficult to eliminate completely.

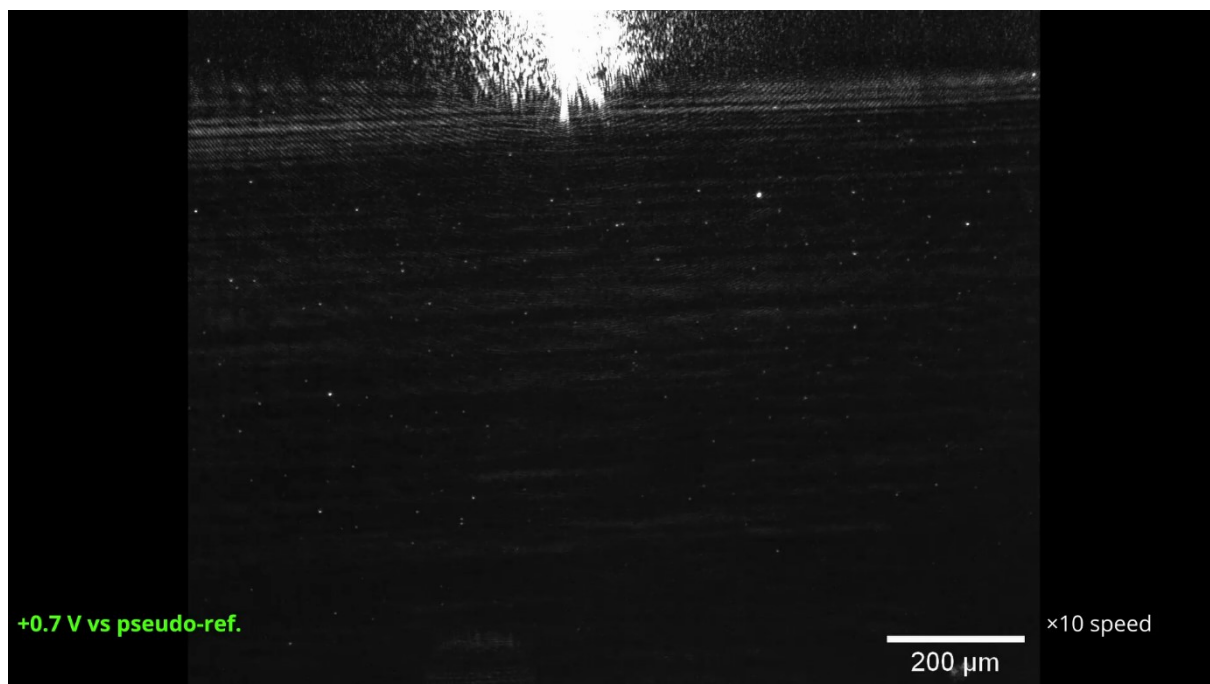


Fig. S5 Snapshot of the video available at <https://doi.org/10.5281/zenodo.18828230>.

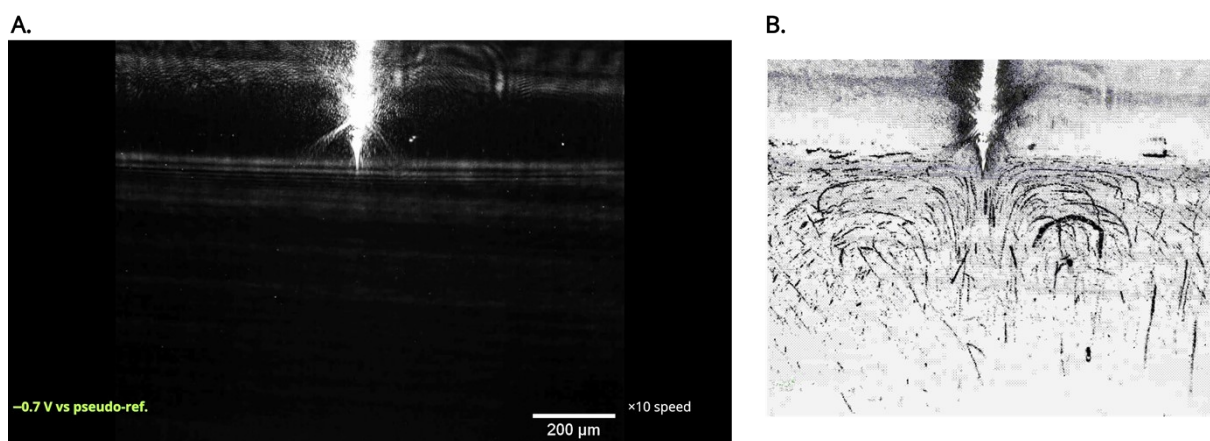
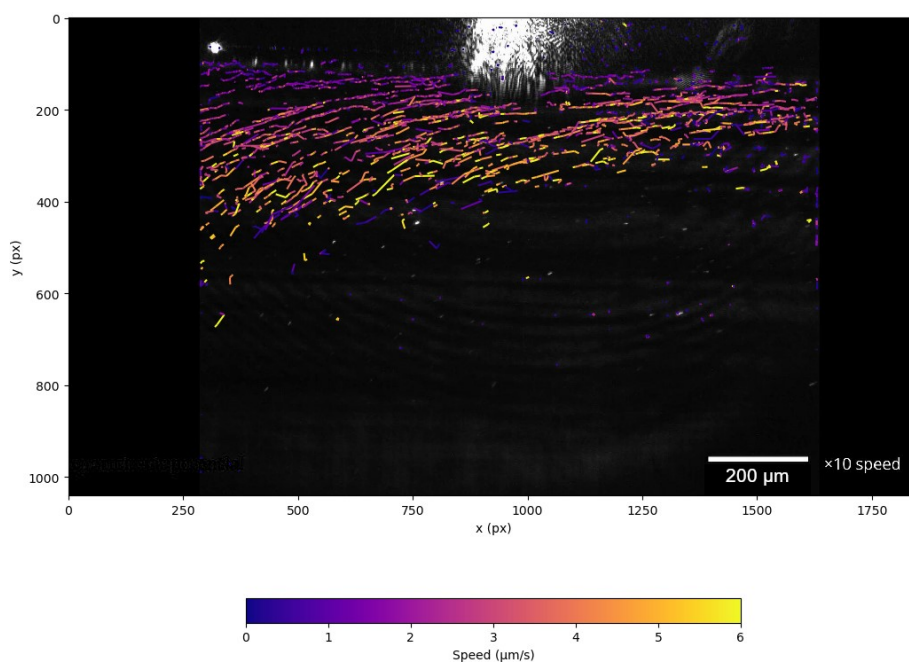


Fig. S6 A. Snapshot of the video available at <https://doi.org/10.5281/zenodo.19905896>. B. Snapshot of the animated GIF available at <https://doi.org/10.5281/zenodo.18828375>.

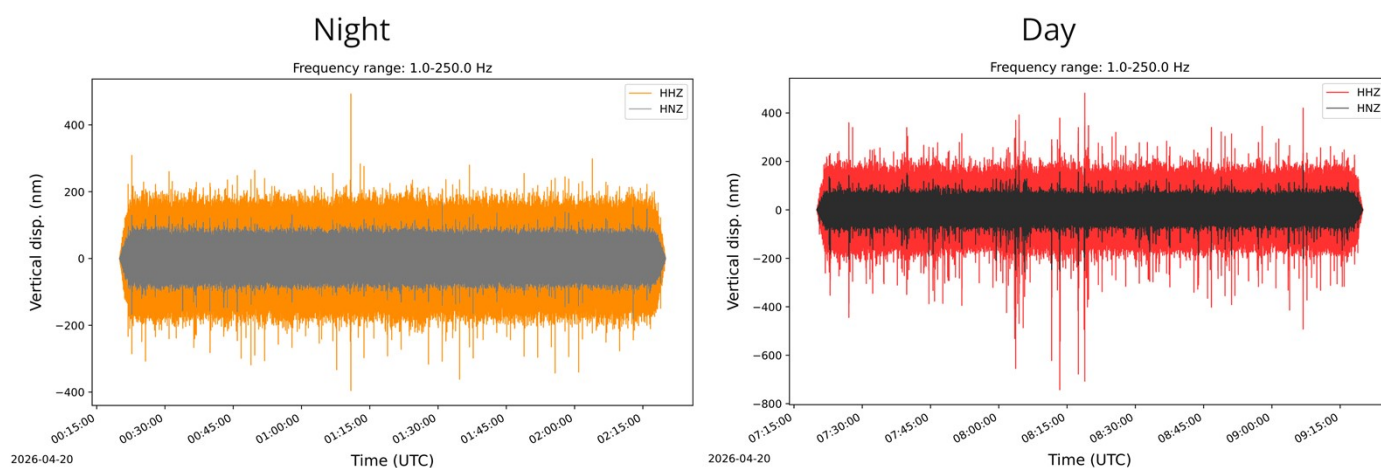
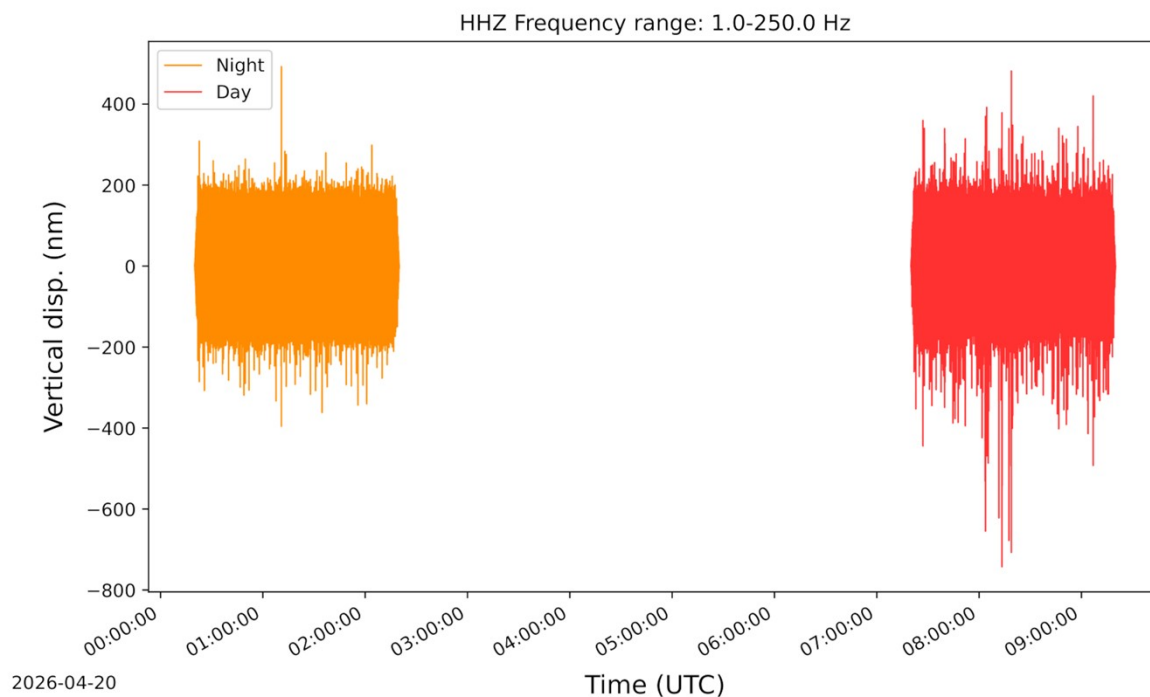
Parasitic convection in the electrochemical cell

When using our experimental setup for observing the trajectories of particles as in Fig. 6 and S4, the experiments were plagued by strong, uneven convection movements in the fluid. It should be kept in mind that Fig. 6 and S4 depict situations where convection was almost inexistent for an exceptionally long duration which allowed us to analyze the particles' trajectories over a long time (190 s) both with and without polarization of the electrode. Most experiments resulted as depicted below, where convection almost dominates and is not constant, forcing us to shorten the duration of the analysis so that convection fluctuations have only a limited impact on the motion of particles.



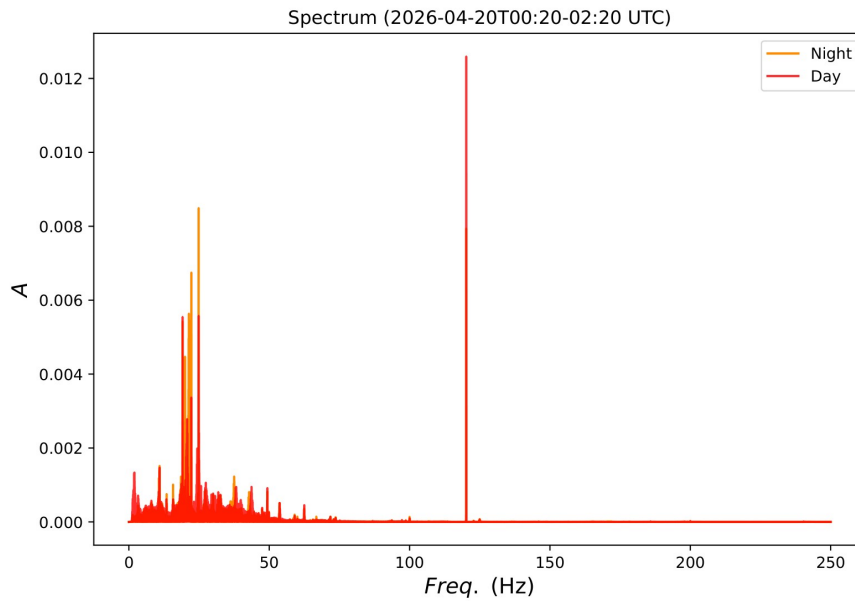
This does not mean that eliminating convection is an irreproducible result, but rather that little to no convection over an extended period of time is a rare event which can be sometimes captured.

As indicated in the main text, we tried to suppress air currents and solvent evaporation. Reducing these sources of thermal gradients (respectively by encasing the setup with thick cardboard panels and adding a few drops of silicon oil to the cell) had a minimal effect on eliminating the convection. Another plausible cause of the fluid movement may be mechanical vibrations. Nonetheless, letting the experiment run overnight, when human activity is largely reduced in the building, did not significantly mitigate the fluid motion. The vertical displacements of the optical setup, measured in the frequency range 1.0–250.0 Hz show no obvious differences with respect to morning time window, few hours later the same day, except for sporadic transient perturbations during the day (see following measurements).



Vertical displacement (in nm) as a function of UTC time during two 2 h time windows (night and day) with a sampling rate of 500 sps (sample per second). Note that due to the small size of the studied aqueous sample, the vibrations susceptible to induce motion in the fluid of the solution have a high-frequency content and are not recorded here due to the sampling rate. Horizontal displacements are not shown but have similar features.

These measurements have been conducted with two high precision seismological sensors (velocimeters) installed in the experimental room on the ground (grey and black traces) and on the experiment table (orange and red traces). The following spectral amplitudes are calculated from the 2 h displacements signals, after subtraction of their mean value:



Since most of the seismic energy is below 100 Hz, except for a striking peak at 120 Hz, there is no clear indication that very high frequency vibrations exist in the experiment room. This suggests that mechanical disturbances are not likely to cause of this parasitic fluid movement. Another source of a local temperature gradient may be the focused heating of the solution with the 5 mW laser used as the illumination source.

We investigated this hypothesis, with inconclusive results. Some experiments consisted in letting the suspension at rest in the dark for dozens of minutes to reach thermal equilibrium and then illuminating the sample with the laser beam. Fluid movement was sometimes visible immediately upon irradiation, while one would expect a constant lag if the laser caused the convection in solution by heating it.

An element that could support the idea of a laser-induced heating is the observation of a recurring global convection movement, where liposomes in the spectroscopy cell had a downward motion when close to the cell window facing the laser beam, and an upward motion when close to the window where the beam exits the cell.

It seems there is a complex interplay of various factors causing this fluid motion.

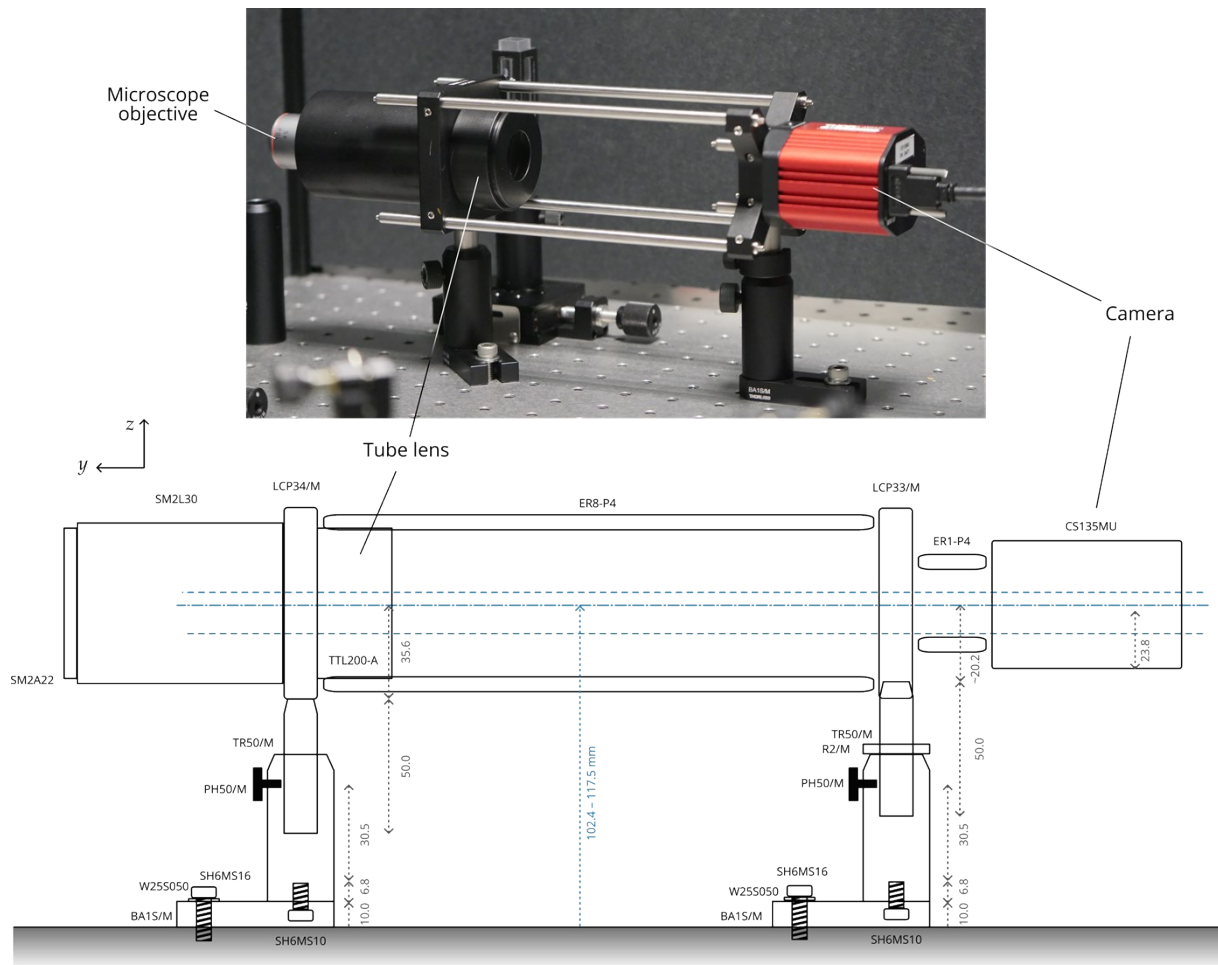


Fig. S7 Horizontal microscope as an observation system consisting of an infinity-corrected $\times 5$ microscope objective, a tube lens and a camera. Thorlabs optical component part references are provided in the diagram, where distances are indicated in mm.

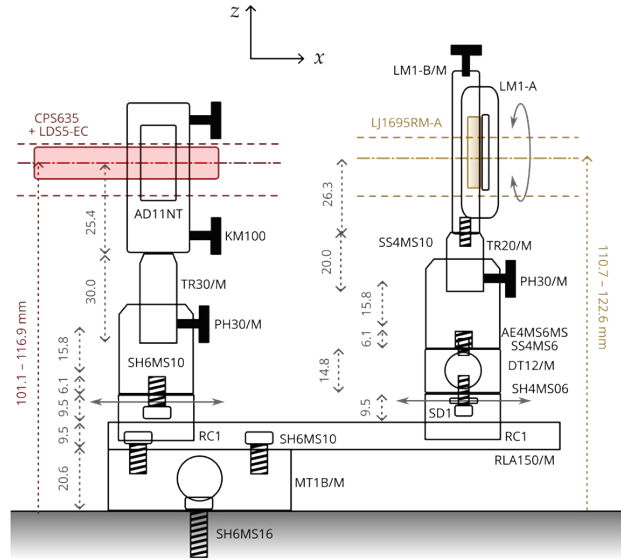
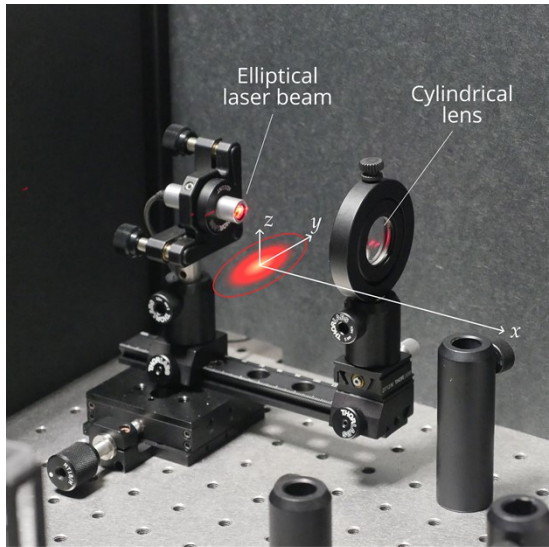


Fig. S8 Illumination system consisting of a laser beam (red) and a lens (brown). Thorlabs optical component part references are provided in the diagram, where distances are indicated in mm.